

The Great Pretenders Among the ULX Class

Dimitris M. Christodoulou^{1,2}, Silas G. T. Laycock^{1,3}, Demosthenes Kazanas⁴, Rigel Cappallo^{1,3}, and Ioannis Contopoulos^{5,6}

¹ Lowell Center for Space Science and Technology, University of Massachusetts Lowell, Lowell, MA, 01854, USA

² Department of Mathematical Sciences, University of Massachusetts Lowell, Lowell, MA, 01854, USA. Email: dimitris.christodoulou@uml.edu

³ Department of Physics & Applied Physics, University of Massachusetts Lowell, Lowell, MA, 01854, USA. Email: silas.laycock@uml.edu, rigelcappallo@gmail.com

⁴ NASA Goddard Space Flight Center, Laboratory for High-Energy Astrophysics, Code 663, Greenbelt, MD 20771, USA. Email: demos.kazanas@nasa.gov

⁵ Research Center for Astronomy and Applied Mathematics, Academy of Athens, Athens 11527, Greece. Email: icontop@academyofathens.gr

⁶ National Research Nuclear University, Moscow 115409, Russia.

Abstract The recent discoveries of pulsed X-ray emission from three ultraluminous X-ray (ULX) sources have finally enabled us to recognize a subclass within the ULX class: the great pretenders, neutron stars (NSs) that appear to emit X-ray radiation at isotropic luminosities $L_X = 7 \times 10^{39} \text{ erg s}^{-1} - 1 \times 10^{41} \text{ erg s}^{-1}$ only because their emissions are strongly beamed toward our direction and our sight lines are offset by only a few degrees from their magnetic-dipole axes. The three known pretenders appear to be stronger emitters than the presumed black holes of the ULX class, such as Holmberg II & IX X-1, IC10 X-1, and NGC300 X-1. For these three NSs, we have adopted a single reasonable assumption, that their brightest observed outbursts unfold at the Eddington rate, and we have calculated both their propeller states and their surface magnetic-field magnitudes. We find that the results are not at all different from those recently obtained for the Magellanic Be/X-ray pulsars: the three NSs reveal modest magnetic fields of about 0.3-0.4 TG and beamed propeller-line X-ray luminosities of $\sim 10^{36-37} \text{ erg s}^{-1}$, substantially below the Eddington limit.

Key words: accretion, accretion disks—stars: magnetic fields—stars: neutron—X-rays: binaries—X-rays: individual (M82 X-2, NGC7793 P13, NGC5907 ULX-1)

1 INTRODUCTION

Ultraluminous X-ray (ULX) sources are extragalactic compact accreting objects characterized by apparent super-Eddington luminosities ($L_X \sim 10^{39-41} \text{ erg s}^{-1}$) and unusual soft X-ray spectra with black-body emission around $\lesssim 0.3 \text{ keV}$ and a downturn above $\sim 3-5 \text{ keV}$ (Gladstone et al. 2009; Feng & Soria 2011; Motch et al. 2014; Middleton et al. 2015). The extreme luminosities observed during outbursts could be understood either as isotropic emission below the Eddington limit ($L_X < L_{Edd} = 1.26 \times 10^{38} M/M_\odot \text{ erg s}^{-1}$) from intermediate-mass ($M \sim 10^{2-4} M_\odot$) black holes or as anisotropic emission with apparent $L_X > L_{Edd}$ from stellar-mass black holes (BHs) and neutron stars (NSs) (Soria 2007; Medvedev & Poutanen 2013; Bachetti et al. 2014; Motch et al. 2014; Pasham et al. 2014).

The former interpretation was not supported by the results of Gladstone et al. (2009) and it is now effectively ruled out by a large number of observations:

- (a) Gilfanov et al. (2004) found that the ULX sources are just the high end of a luminosity function that cuts off at $L_X \sim 3 \times 10^{40}$ erg s $^{-1}$ and in which the known high-mass X-ray binaries (HMXBs) make up the low end of a single power-law with slope ~ 1.6 .
- (b) Liu et al. (2013) determined from optical spectroscopy that the mass of the compact object in M101 ULX-1 is no more than $30M_\odot$. It is unlikely that this is an intermediate-mass BH.
- (c) Luangtip et al. (2014) analyzed a *Chandra* sample of nearby ULX sources and found a change in the spectral index around $L_X \sim 2 \times 10^{39}$ erg s $^{-1}$ that may indicate a transition to the apparent super-Eddington accretion regime by $10M_\odot$ BHs or to strongly anisotropic emission from NSs. This result was confirmed by the independent study of Sutton et al. (2017).
- (d) Bachetti et al. (2014) determined that the ULX source X-2 in M82 harbors a pulsar with spin period $P_S = 1.3725$ s and spinup rate $\dot{P}_S = -2 \times 10^{-10}$ s s $^{-1}$.
- (e) Motch et al. (2014) determined that the ULX source P13 in NGC7793 harbors a stellar-mass compact object with $M < 15 M_\odot$. Pulsations were next detected from this source (Fürst et al. 2016; Israel et al. 2017b), so now we know that the compact object is a NS with $P_S = 0.417$ s and an average $\dot{P}_S = -3.5 \times 10^{-11}$ s s $^{-1}$.
- (f) Laycock et al. (2015) determined from the radial velocity curve of IC10 X-1 that the the compact object could be a NS, although a low-stellar-mass BH cannot be ruled out.
- (g) Israel et al. (2017a) detected pulsations from NGC5907 ULX-1, so this is the third object of the class harboring a NS with $P_S = 1.137$ s and an average $\dot{P}_S = -8.1 \times 10^{-10}$ s s $^{-1}$. This is also the most luminous and the most distant NS pretender ever detected, given its apparent luminosity of $L_X = 10^{41}$ erg s $^{-1}$ and a distance to the source of $D = 17.1$ Mpc.

The magnetic field of NGC7793 P13 has been recently estimated to be $B \approx 1.5$ TG (Fürst et al. 2016), and in the case of M82 X-2, Bachetti et al. (2014) used their measurement of the accretion torque to obtain a modest value of the magnetic field $B \approx 1$ TG. Somewhat higher values were obtained by Israel et al. (2017a) for the magnetic field of NGC5907 ULX-1 in which these authors also analyzed the possibility of multipolar fields on the surface of the NS (see also Chen 2017, for a similar analysis in the case of M82 X-2). As we shall see below, such assumptions may not be necessary as the faint X-ray states and the magnetic fields of these NSs are determined to be quite modest and in strong agreement with the estimates of King & Lasota (2016) for M82 X-2 and with the estimates of Christodoulou et al. (2016) for several Magellanic HMXBs.

More evidence keeps piling up that the magnetic fields of the ULX objects are not exotic. For instance, Brightman et al. (2016), based on *NuSTAR* observations of M82 X-2, found a spectral cutoff at 14_{-3}^{+5} keV which implies a 1.2 TG surface magnetic field. On the other hand, Tsygankov et al. (2016) and Dall’Osso et al. (2016) have interpreted the faintest states of M82 X-2 as low-level emission that occurs due to leakage and continued accretion of matter when the system moves into the Corbet (1996) gap. As we shall see below, this interpretation that leads to higher magnetic-field values is not supported by the theory or the observations of the other two pretenders.

In Section 2, we calculate the physical properties of the faintest accreting states of the three NS pretenders (their so-called “propeller” states) that lie at anisotropic X-ray luminosities of $\sim 10^{36-37}$ erg s $^{-1}$. We adopt a single reasonable assumption, that the brightest radiation seen from these NSs is beamed emission that proceeds at the Eddington rate¹ (despite the observed spread of more than an order of magnitude in the highest X-ray luminosities of these sources). In that respect, the outbursts of these sources are not at all dissimilar from the type-II outbursts of Magellanic Be/X-ray pulsars that have been observed to rise up to the Eddington limit (Coe et al. 2010; Christodoulou et al. 2016, their Figures 2 and 4). Then we show that at their faintest accreting states, these objects appear to be very similar and typical NSs; emitting anisotropically modest amounts of radiation; and supporting modest surface mag-

¹ This assumption is supported by the recent simulations of anisotropic outflows from NS accretion columns by Kawashima et al. (2016).

Table 1 NS ULX Measurements

Source Name	L_{max} (erg/s)	L_{min} (erg/s)	P_S (s)	\bar{P}_S (s s $^{-1}$)	D (Mpc)
NGC7793 P13	7×10^{39}	5×10^{37}	0.417	-3.5×10^{-11}	3.6 or 3.9
NGC5907 ULX-1	1×10^{41}	3×10^{38}	1.137	-8.1×10^{-10}	17.1
M82 X-2	2×10^{40}	1×10^{38}	1.3725	-2.0×10^{-10}	3.6

References.—NGC7793 P13: Motch et al. (2014), Fürst et al. (2016), Israel et al. (2017b). NGC5907 ULX-1: Israel et al. (2017a). M82 X-2: Bachetti et al. (2014), Brightman et al. (2016).

Table 2 NS ULX Estimates

Source Property	NGC7793 P13	NGC5907 ULX-1	M82 X-2	Input Parameters
$L_{max}(10^{40} \text{ erg/s})$	0.7	10	2	Values from Table 1
$L_{Edd}(10^{38} \text{ erg/s})$	1.8	1.8	1.8	For $M = 1.4 M_\odot$
Beaming Factor b	38.9	556	111	$= L_{max}/L_{Edd}$, eq. (1)
Half-Opening Angle $\theta_{\frac{1}{2}}(^o)$	18	5.0	11	$= 114.6/\sqrt{b}$, eq. (2)
$L_{iso}(10^{39} \text{ erg/s})$	0.50	1.1	0.18	P_S and \bar{P}_S in eq. (3) with $\eta = 0.5$
$L_{prop}(10^{36} \text{ erg/s})$	13	2.0	1.6	$= L_{iso}/b$, eq. (4)
B (TG)	0.29	0.37	0.41	P_S and L_{prop} in eqs. (5) and (6)
$L_{min}/b(10^{36} \text{ erg/s})$	1.3	0.54	0.90	L_{min} from Table 1 and b

Error Bars.—Not accounting for errors in the distances to the sources, the errors determined from the observations in Table 1 are as follows (left to right): $\Delta(\ln P_S) = 4.8 \times 10^{-6}, 3.5 \times 10^{-6}, 8.7 \times 10^{-8}$; $\Delta(\ln \bar{P}_S) = 8.6 \times 10^{-4}, 1.2 \times 10^{-2}, 6.9 \times 10^{-3}$; and $\Delta(\ln L_{max}) = 0.015, 0.20, 0.12$. The calculated errors are as follows (left to right): $\Delta(\ln L_{iso}) = 8.6 \times 10^{-4}, 1.2 \times 10^{-2}, 6.9 \times 10^{-3}$; and $\Delta(\ln b) = \Delta(\ln[L_{min}/b]) = \Delta(\ln L_{prop}) = 0.015, 0.20, 0.12$.

netic fields; properties that are quite similar to those also found for the propeller emission states of the Magellanic Be/X-ray pulsars. In Section 3, we discuss and summarize our results.

2 THE PROPELLER STATES OF THE THREE PRETENDERS

In Table 1, we summarize the recent measurements of the properties of the three NS pretenders. Two trends appear to be common for the group:

- (1) The NSs are spinning up over times that span 18 days (M82 X-2) to 4–12 years (12 years in the case of NGC5907 ULX-1; Israel et al. 2017a). This indicates that accretion of matter with high specific angular momentum spins up these pulsars while, at the same time, changes in the magnetospheres (such as the opening of magnetic-field lines and the electric currents flowing along open lines) are not able to generate strong enough retarding torques² to reverse this secular trend (Harding et al. 1999; Contopoulos et al. 1999, 2014).
- (2) The lowest observed X-ray luminosities L_{min} are deceptively close to the Eddington limit for the canonical $1.4 M_\odot$ pulsar. But we cannot trust this trend to be more than a coincidence because we do not know whether these L_{min} values represent faint accreting states or faint magnetospheric emission (Campana et al. 1995; Campana 1997), since pulsations have not been detected in these observa-

² Using eq. (18) in Contopoulos et al. (2014), the measured values of P_S , and the below-determined values of B , we find that the spin-down rates for the pretenders are $\dot{P}_{SD} = 0.82\pi^2 B^2 R^6/(c^3 I P_S) \sim 10^{-17} \text{ s s}^{-1}$, values that are clearly negligible as compared to the measured spin-up rates listed in Table 1. Here c is the speed of light and R and I are the canonical values of the NS radius and moment of inertia, respectively. For pulsars such as the pretenders with $P_S \sim 1 \text{ s}$, this estimate can be increased by a factor of $(R_{lc}/R_{co})^2 \sim 10^3$ depending on the locations of the corotation radius R_{co} and the light-cylinder radius R_{lc} (Contopoulos 2005), but still the resulting spin-down rates are orders of magnitude smaller than the observed spin-up rates. It appears then that in pulsars with $P_S \sim 1 \text{ s}$, the inward push of the accretion disks cannot disrupt the magnetospheres enough to affect strong electromagnetic spin-down.

tions. The nature of these states can be revealed after the nature of the brightest states L_{max} is deciphered (see below).

We carry out a sequence of calculations that we also summarize in the rows of Table 2. We begin with the extreme values of the observed X-ray luminosities L_{max} (Table 1) which we introduce in the first row of Table 2. As many other researchers have stated in the past, we believe that these luminosities cannot indicate isotropic emissions from these pulsars—instead, the radiation must be strongly beamed toward our direction. But we do realize that the sources displaying these L_{max} values are undergoing powerful collimated outbursts, in which case it is reasonable to assume that the emitted radiation is limited by the Eddington rate in all cases (see also footnote 1). We also adopt canonical pulsar parameters (mass $M = 1.4M_\odot$ and radius $R = 10$ km) throughout the derivations. Then $L_{Edd} = 1.8 \times 10^{38}$ erg s $^{-1}$, and we can calculate the beaming factors of the emitted X-rays which we define here as

$$b \equiv \frac{L_{max}}{L_{Edd}} > 1. \quad (1)$$

The beaming factors for critical accretion give us an idea about the half-opening angles $\theta_{\frac{1}{2}}$ of the collimated emissions. The solid angles are $4\pi/b$ steradians and then the half-opening angles of the emission cones $\theta_{\frac{1}{2}}$ are given by $\pi(\theta_{\frac{1}{2}})^2 = 4\pi/b$, viz.

$$\theta_{\frac{1}{2}} = \left(\frac{360}{\pi} \right) b^{-1/2} \text{ deg.} \quad (2)$$

We find that $\theta_{\frac{1}{2}}$ varies between 5 and 18 degrees, where the most stringent value corresponds to the most luminous outburst (NGC5907 ULX-1 in Table 2). This value is in agreement with the range of $\theta_{\frac{1}{2}} = 5.0\text{--}6.7$ degrees found for this source by Dauser et al. (2017) who produced a model with a slightly precessing inflow and outflow and strong beaming. The accretion in this model is however supercritical and the maximum anisotropic luminosity emitted in the funnel is found to be in the range of $(5\text{--}8)L_{Edd}$. Nevertheless, the model of Dauser et al. (2017) is important because it shows that a slight precession of the outflow can reproduce the nearly sinusoidal pulse profiles observed in the NS pretenders. The shape of the pulse profiles was used in the past to raise objections against strong beaming (Bachetti et al. 2014; Brightman et al. 2016; Fürst et al. 2016, among others), but now it does not appear to be a problem.

Next we use the measured values of P_S and \dot{P}_S (Table 1) to find the isotropic X-ray luminosities L_{iso} of the NSs in their faintest accreting states (Appendix B in Galache et al. 2008; Frank et al. 2002), viz.

$$L_{iso} = \frac{1}{2} \eta (2\pi I |\dot{P}_S|) \left(\frac{2\pi}{P_S^7} \frac{GM}{R^3} \right)^{1/3}, \quad (3)$$

where I is the canonical moment of inertia, G is the gravitational constant, and we introduced an additional factor of $\eta/2$ for the efficiency of converting accretion power to X-rays (η taken here to be 0.5). The leading factor of 1/2 applies specifically to collimated outflows from NSs (Körding et al. 2006) and it implies an effective NS conversion efficiency of $\eta/2 = 0.25$. The introduction of $\eta/2$ also implies that we assume that minimum accretion takes place at a reduced torque than the observed maximum value. In the case of M82 X-2, this is certainly true because the observed value of \dot{P}_S was obtained only at outburst and for a very limited time span of 18 days (Fig. 2a in Bachetti et al. 2014).

Next the isotropic “propeller” luminosities L_{iso} are scaled by b and the true anisotropic X-ray luminosities

$$L_{prop} = \frac{L_{iso}}{b}, \quad (4)$$

are obtained for collimated emission in the propeller states (see Table 2). The faintest observed isotropic luminosities L_{min} shown in Table 1 are also scaled by b and they are introduced at the bottom of Table 2 for comparison purposes.

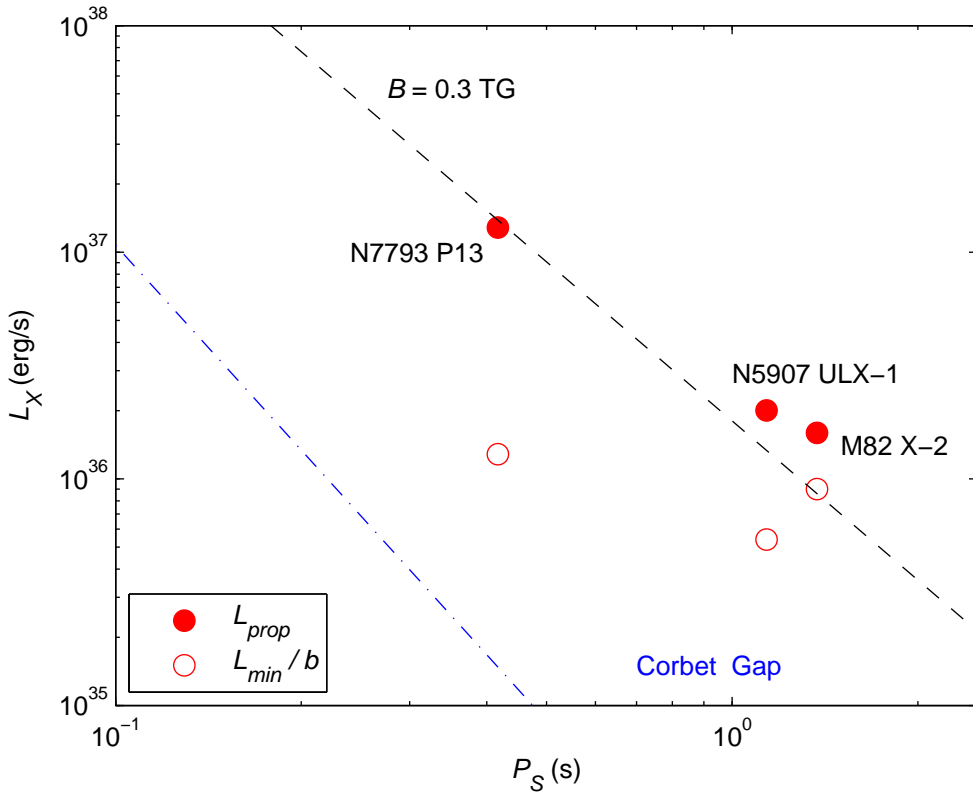


Fig. 1 The anisotropic propeller states (i.e., the faintest accreting states; solid circles) and the faintest anisotropic states observed (open circles) in $P_S - L_X$ space for the three NS pretenders. The data points come from Tables 1 and 2. Errors are given in Table 2; error bars are very small for P_S and about the size of the circles for L_X (smaller for NGC7793 P13). The dashed line is the lowest propeller line with $B = 0.3$ TG found for the Magellanic Be/X-ray pulsars (Christodoulou et al. 2016). Comparison indicates that the surface magnetic fields of these NSs are modest ($B \approx 0.3\text{--}0.4$ TG). The dashed-dotted line with a slope of -3 specifies the lower boundary of the Corbet (1996) gap for the $B = 0.3$ TG propeller line.

Finally, a minimum value for the surface magnetic field B is estimated from the standard equation of Stella et al. (1986) for the propeller line, viz.

$$L_{prop} = 2 \times 10^{37} \left(\frac{\mu}{10^{30} \text{ G cm}^3} \right)^2 \left(\frac{P_S}{1 \text{ s}} \right)^{-7/3} \text{ erg s}^{-1}, \quad (5)$$

where canonical pulsar parameters have been used and the magnetic moment is defined by

$$\mu \equiv BR^3. \quad (6)$$

This equation does not depend on P_S , thus it does not rely on torque balance at the inner edge of the accretion disk and it does not use the conservation of angular momentum (Frank et al. 2002) in the determination of the magnetic field.

The results for L_{prop} summarized in Table 2 are plotted in the $P_S - L_X$ diagram in Figure 1 as filled circles. We see now that these three pulsars are totally nonexotic, sporting propeller luminosities

in the range of $L_{prop} \sim 10^{36-37}$ erg s $^{-1}$ and surface magnetic fields in the range of $B \approx 0.3\text{-}0.4$ TG. In these respects, the pretenders are not at all dissimilar from the short-period HMXBs found in the Magellanic Clouds and studied under the assumption of isotropic emission (Christodoulou et al. 2016). In fact, several of the Magellanic sources also appear to rise up during powerful type-II outbursts to just about the Eddington limit, an observation that is responsible for our adoption of this assumption in the present work.

The B -values found for the three pretenders are in agreement with the results obtained by King & Lasota (2016) for M82 X-2 and other accreting NSs that exhibit beamed emission at the apparent level of $L_{max} \sim 10^{40}$ erg s $^{-1}$. The importance of our results is that they predict similar modest values and properties for NS ULX sources that appear to radiate at a much higher level of power (see NGC5907 ULX-1 in Table 2).

The faintest anisotropic states L_{min}/b of the three pretenders shown in Table 2 are also plotted in Figure 1 as open circles. For the measured spin periods, these states fall within the Corbet (1996) gap which suggests that we have observed weak magnetospheric emission in the absence of accretion (Campana et al. 1995; Campana 1997). The case for NGC7793 P13 is especially strong: the faintest observation (Motch et al. 2014) lies one order of magnitude below the propeller value of $L_{prop} = 1.3 \times 10^{37}$ erg s $^{-1}$. On the other hand, the faintest observation of M82 X-2 (Brightman et al. 2016) lies only a factor of ~ 2 below the propeller value $L_{prop} = 1.6 \times 10^{36}$ erg s $^{-1}$. But for this pulsar there exists an independent confirmation of its propeller value: From 15 years of *Chandra* observations, Tsygankov et al. (2016) found that M82 X-2 has repeatedly switched between its high isotropic state L_{max} and a low isotropic state with $L_{iso} = 1.7 \times 10^{38}$ erg s $^{-1}$ (see also Dall'Osso et al. 2016, who obtained the same value as an upper limit). Using $b = 111$ (Table 2), this faint state corresponds to $L_{prop} = 1.5 \times 10^{36}$ erg s $^{-1}$ in strong agreement with our determination of the propeller value derived from beaming of the L_{max} value of this source. It seems then that M82 X-2 has bounced for many years between its propeller state and its ultraluminous state. This agreement between results consolidates the physical properties of M82 X-2 listed in Table 2.

3 SUMMARY AND DISCUSSION

We have used standard accretion theory and beaming of the X-ray emission (Stella et al. 1986; Frank et al. 2002; Galache et al. 2008; King & Lasota 2016) in order to estimate the typical values of the minimum anisotropic luminosities and the surface magnetic fields of the three recently discovered ULX pulsars (Table 1; Bachetti et al. 2014; Fürst et al. 2016; Israel et al. 2017a,b). For the measured values of L_{max} , P_S , and \dot{P}_S , our results show that the physical and geometric parameters are all modest (Table 2) and not at all dissimilar (Fig. 1) from those found for the entire sample of the short-period ($P_S < 100$ s) Magellanic HMXBs (Christodoulou et al. 2016). The three modest NSs only pretend to emit at enormous super-Eddington rates because their emissions are collimated and our sight lines are close to their magnetic-dipole axes (Section 2).

Since the X-rays originate from a limited region around the magnetic poles, we can estimate the sizes r and temperatures T of these hot spots during the faintest accretion states in which the corotation radius is comparable to the magnetospheric radius. The radii of the hot spots are approximately given by $r = R \sqrt{R/R_{co}}$, where R_{co} is the corotation radius; and then the temperatures are $T = [L_{Edd}/(\sigma\pi r^2)]^{1/4}$, where σ is the Stefan-Boltzmann constant. Using the values listed in Table 1, we find that typically $r = 1.0 - 0.7$ km and $T = (1.0 - 1.2) \times 10^8$ K corresponding to photon energies of $kT = 8.5 - 10.4$ keV at the bases of the outflows. Such temperatures may be sufficient for the production of particle pairs that can cross magnetic-field lines and escape along the magnetic axes in mildly relativistic outflows that help increase the effective opening angles of the emission cones listed in Table 2.

Furthermore, if the emissions from the pretenders are collimated, some of the energy must emerge at much longer wavelengths. This appears to be the case for M82 X-2 according to the radio observations of Kronberg et al. (1985), McDonald et al. (2002), and Fenech et al. (2008); and the infrared observations of Kong et al. (2007) and Gandhi et al. (2011). The radio maps show a core-dominated source which is expected if the pulsar is a modestly aligned rotator and a collimated jet is coming out in our direction.

Kong et al. (2007) also produced *Chandra* X-ray spectra that are hard (photon indices $1.3 - 1.7$ from an absorbed power-law model) and show no soft excess. This, combined with the strong X-ray variability on timescales of ~ 2 months and the recurring type-II outbursts, indicates that M82 X-2 is not at all dissimilar from Galactic and Magellanic X-ray binaries harboring NSs (Yang et al. 2017). The recent X-ray observations reported by Brightman et al. (2016) and Tsygankov et al. (2016) for M82 X-2 have effectively confirmed this picture.

In the Magellanic Clouds, two HMXBs have been observed each during two major type-II outbursts³ with apparent $L_{max} > L_{Edd}$: LXP8.04 (Edge et al. 2004; Vasilopoulos et al. 2014; Tendulkar et al. 2014) and SMC X-2 (Laycock et al. 2005; Kennea et al. 2015). As summarized by Christodoulou et al. (2016), the brightest bursts reached luminosities of $L_{max} = 8 \times 10^{38}$ erg s $^{-1}$ (LXP8.04, $D = 50$ kpc) and $L_{max} = 4 \times 10^{38}$ erg s $^{-1}$ (SMC X-2, $D = 60$ kpc) that reveal small beaming factors (eq. [1]) of about 2.2 and 4.4, respectively. These very small degrees of beaming (half-opening angles of $\theta_{\frac{1}{2}} = 77^\circ$ and 54° , respectively; eq. [2]) and our orientation within such wide emission cones account for the differences in the light curves and the spectral features between these most extreme HMXBs and the strongly beaming NS pretenders. The ULX spectral features are discussed below.

The main properties of the so-called ultraluminous state (Gladstone et al. 2009; Feng & Soria 2011; Motch et al. 2014; Middleton et al. 2015; Kobayashi et al. 2017) are:

1. A soft blackbody (BB) excess at $\lesssim 0.3$ keV. It is believed that this could be emission from the accretion disk.
2. A downturn of the spectrum at $\sim 3\text{-}5$ keV. This is consistent with our calculation of photon energies of $kT = 8.5 - 10.4$ keV at the bases of the outflows. Operating at $L_{max}/b = L_{Edd}$, the sources would not be able to produce more energetic photons in substantial numbers. A large number of photons is also capable of escaping from the sides of the accretion column (Kawashima et al. 2016; Basko & Sunyaev 1976) in a fan-like configuration and most of them do not reach the observer if our sight lines are oriented close to the magnetic-dipole axes, as in the case of the pretenders.
3. Featureless spectra with no emission/absorption lines. This implies that the X-rays are not reprocessed in the surrounding medium, that is they find holes in a clumpy medium to shine through (as was found by Kobayashi et al. 2017, in *Suzaku* observations of Holmberg IX X-1).
4. A power law at the hard part of the spectrum. Comptonization of the primary (unprocessed) photons from the source may be responsible for this component.
5. The soft part is often fitted well by two-color disk BB models. Multi-color BB models could be revealing the spectrum of a cooler wind outflow emanating in the emission funnel (see also Walton et al. 2016).
6. No cyclotron resonance features. This can be explained by the weak magnetic fields of the pretenders. For the determined values of $B = 0.3\text{-}0.4$ TG, such lines may only emerge at 3.5-4.6 keV which is the area of the spectrum downturn.

Urquhart & Soria (2016) observed eclipses in two ULX sources in M51. For these sources, $L_{max} \approx 2 \times 10^{39}$ erg s $^{-1}$, substantially lower than the L_{max} values of the pretenders and slightly below the empirical critical value of $L_{crit} \sim 3 \times 10^{39}$ erg s $^{-1}$ (Luangtip et al. 2014; Sutton et al. 2017) that apparently subdivides the central engines of the ULX sources into stellar-mass BHs and NS pretenders. Since our line of sight is very much inclined to the magnetic axes of both of these eclipsing binaries, the radiation cannot be beamed at all. We conclude that both of these sources contain stellar-mass BHs with masses $M_{BH} \gtrsim 16M_\odot$ radiating isotropically at about the Eddington rate ($L_{max} \lesssim L_{Edd}$). Objects such as these reinforce our belief that the NSs of the ULX class only pretend to radiate more power than the BHs of the class. In this respect, weaker sources with $L_{max} \sim 2 \times 10^{38}$ erg s $^{-1}$, such as IC10 X-1 (Laycock et al.

³ A type-II outburst of SMC X-3 was recently reported by Weng et al. (2017) and Tsygankov et al. (2017) and it was monitored by *Swift/XRT* and *NuSTAR*. For this HMXB, the observations indicate that $L_{max} = 2.5 \times 10^{39}$ erg s $^{-1}$ and $L_{min} = 3.0 \times 10^{34}$ erg s $^{-1}$ ($D = 62$ kpc; Tsygankov et al. 2017). Assuming that this event was due to critical accretion at the Eddington rate, we find that we need modest beaming ($b = 14$ and $\theta_{\frac{1}{2}} = 31^\circ$), the minimum beamed luminosity L_{min}/b falls in the middle of the Corbet gap, and the dipolar magnetic field on the surface of the NS is $B = 1.1$ TG.

2015) and NGC300 X-1 (Binder et al. 2011), that bridge the gap between HMXBs and ULX sources may not contain BHs (their masses would have to be no more than $2M_{\odot}$), so they could also contain NSs; otherwise most of the radiation is beamed away from our direction (IC10 X-1 is an eclipsing binary); or accretion is markedly suppressed in these objects, perhaps for some of the reasons recently put forth by Tutukov & Fedorova (2016).

Acknowledgements We thank an anonymous referee for suggestions that led to improvements and clarifications in the paper. DMC, SGTL, and RC were supported by NASA grant NNX14-AF77G. DK was supported by a NASA ADAP grant.

References

Bachetti, M., Harrison, F. A., Waltron, D. J., et al. 2014, *Nature*, 514, 202
 Basko, M. M., & Sunyaev, R. A. 1976, *MNRAS*, 395, 417
 Beloborodov, A. M. 2002, *ApJ*, 566, L85
 Binder, B., Williams, B. F., Eracleous, M., et al. 2011, *ApJ*, 742, 128
 Brightman, M., Harrison, F., Walton, D. J., et al. 2016, *ApJ*, 816, 60
 Campana, S. 1997, *A&A*, 320, 840
 Campana, S., Stella, L., Mereghetti, S., & Colpi, M. 1995, *A&A*, 297, 385
 Chen, W.-C. 2017, *MNRAS*, 465, L6
 Christodoulou, D. M., Laycock, S. G. T., Yang, J., & Fingerman, S. 2016, *ApJ*, 829, 30
 Coe, M. J., McBride, V. A., & Corbet, R. H. D. 2010, *MNRAS*, 401, 252
 Contopoulos, I. 2005, *A&A*, 442, 579
 Contopoulos, I., Kalapotharakos, C., & Kazanas, D. 2014, *ApJ*, 781, 46
 Contopoulos, I., Kazanas, D., & Fendt, C. 1999, *ApJ*, 511, 351
 Corbet, R. H. D. 1996, *ApJ*, 457, L31
 Dall'Osso, S., Perna, R., Papitto, A., et al. 2016, *MNRAS*, 457, 3076
 Dauser, T., Middleton, M., & Wilms, J. 2017, *MNRAS*, 466, 2236
 Edge, W. R. T., Coe, M. J., Galache, J. L., & Hill, A. B. 2004, *MNRAS*, 349, 1361
 Fenech, D. M., Muxlow, T. W. B., Beswick, R. J., et al. 2008, *MNRAS*, 391, 1384
 Feng, H., & Soria, R. 2011, *New Astr. Rev.*, 55, 166
 Frank J., King A., & Raine D. 2002, *Accretion Power in Astrophysics*, 3rd Edition, Cambridge: Cambridge University Press
 Fürst, F., Walton, D. J., Harrison, F. A., et al., 2016, *ApJ*, 831, L14
 Galache, J. L., Corbet, R. H. D., Coe, M. J., Laycock, S., & Schurch, M. P. E., 2008, *ApJS*, 177, 189
 Gandhi, P., Isobe, N., Birkinshaw, M., et al., 2011, *PASJ*, 63, S505
 Gilfanov, M., Grimm, H.-J., Sunyaev, R., 2004, *Nuc. Phys. Suppl.*, 132, 369
 Gladstone, J. C., Roberts, T. P., & Done C. 2009, *MNRAS*, 397, 1836
 Harding, A. K., Contopoulos, I., & Kazanas, D. 1999, *ApJ*, 525, L125
 Israel, G. L., Belfiore, A., Stella, L., et al., 2017a, *Science*, 355, 817, arXiv:1609.07375
 Israel, G. L., Papitto, A., Esposito, P., et al., 2017b, *MNRAS*, 466, L48
 Kawashima, T., Mineshige, S., Ohsuga, K., & Ogawa, T. 2016, *PASJ*, 68, 83
 Kennea, J. A., Burrows, D. N., Coe, M. J., et al. 2015, *ATel*, 8091, 1
 King, A., & Lasota, J.-P. 2016, *MNRAS*, 458, L10
 Kobayashi, S. B., Nakazawa, K., & Makishima, K. 2017, *PASJ*, 69, 4
 Kong, A. K. H., Yang, Y. J., Hsieh, P.-Y., Mak, D. S. Y., & Pun, C. S. J. 2007, *ApJ*, 671, 349
 Körding, E. G., Fender, R. P., & Migliari, S. 2006, *MNRAS*, 369, 1451
 Kronberg, P. P., Biermann, P., & Schwab, F. R. 1985, *ApJ*, 291, 693
 Laycock, S., Corbet, R. H. D., Coe, M. J., et al. 2005, *ApJS*, 161, 96
 Laycock, S. G. T., Maccarone, T. J., & Christodoulou, D. M. 2015, *MNRAS*, 452, L31
 Liu, J.-F., Bregman, J. N., Bai, Y., et al. 2013, *Nature*, 503, 500
 Luangtip, W., Roberts, T. P., Mineo, S., et al. 2014, in *The X-ray Universe 2014*, J.-U. Ness (ed.), http://xmm.esac.esa.int/external/xmm_science/workshops/2014symposium/, id. 120

McDonald, A. R., Muxlow, T. W. B., Wills, K. A., et al. 2002, MNRAS, 334, 912
Medvedev, A. S., & Poutanen, J. 2013, MNRAS, 431, 2690
Middleton, M. J., Heil, L., Pintore, F., et al. 2015, MNRAS, 447, 3243
Motch, C., Pakull, M. W., Soria, R., et al. 2014, Nature, 514, 198
Pasham, D. R., Strohmayer, T. E., & Mushotzky, R. F. 2014, Nature, 513, 74
Soria, R. 2007, in Black Holes from Stars to Galaxies - Across the Range of Masses, V. Karas & G. Matt (eds.), Proc. IAU Symp., 238, p. 235
Stella, L., White, N. E., & Rosner, R. 1986, ApJ, 308, 669
Sutton, A. D., Swartz, D. A., Roberts, T. P., et al. 2017, ApJ, 836, 48
Tendulkar, S. P., Fürst, F., Pottschmidt, K., et al. 2014, ApJ, 795, 154
Tsygankov, S. S., Doroshenko, V., Lutovinov, A. A., et al. 2017, A&A, submitted, arXiv: 1702:00966
Tsygankov, S. S., Mushtukov, A. A., Suleimanov, V. F., & Poutanen, J. 2016, MNRAS, 457, 1101
Tutukov, A. V., & Fedorova, A. V. 2016, ARep, 60, 106
Urquhart, R., & Soria, R. 2016, ApJ, 831, 56
Vasilopoulos, G., Haberl, F., Sturm, R., et al. 2014, A&A, 567, A129
Walton, D. J., Middleton, M. J., Pinto, C., et al. 2016, ApJ, 826, L26
Weng, S.-S., Ge, M.-Y., Zhao, H.-H., et al. 2017, ApJ, submitted, arXiv: 1701:02983
Yang, J., Laycock, S. G. T., Christodoulou, D. M., et al. 2017, ApJS, in press